

Thermal Production of Charmonia in Pb-Pb Collisions at $\sqrt{s_{NN}} = 5.02$ TeV

Baoyi Chen^{1,2}

¹*Department of Physics, Tianjin University, Tianjin 300350, China*

²*Institut für Theoretische Physik, Goethe-Universität Frankfurt,
Max-von-Laue-Str. 1, D-60438 Frankfurt am Main, Germany*

(Dated: September 23, 2019)

This work studies the thermal production of J/ψ and $\psi(2S)$ with Boltzmann transport model in the Quark Gluon Plasma (QGP) produced in $\sqrt{s_{NN}} = 5.02$ TeV Pb-Pb collisions. J/ψ nuclear modification factors are studied in details with the mechanisms of primordial production and the recombination of charm and anti-charm quarks in the thermal medium. $\psi(2S)$ binding energy is much smaller in the hot medium compared with the ground state, so $\psi(2S)$ with middle and low p_T can be mainly thermally regenerated in the later stage of QGP expansions which enables $\psi(2S)$ inherit larger collective flows from the bulk medium. We quantitatively study both nuclear modification factors of J/ψ and $\psi(2S)$ in different centralities and transverse momentum bins in $\sqrt{s_{NN}} = 5.02$ TeV Pb-Pb collisions.

I. INTRODUCTION

Heavy flavors due to their large masses, have unique advantages in both experimental and theoretical studies of Quantum Chromo-Dynamics (QCD). Since J/ψ was proposed as a probe of the deconfined matter called “Quark-gluon Plasma” (QGP) [1], its yield abnormal suppression by partons and new enhancement from the recombination of charm and anti-charm quarks in QGP have been widely studied in experiments [2–5] and theoretical models [6–12]. Charmonium produced by initial hard process labelled as “primordial production” at the hadronic collisions scatters with nucleon spectators [13]. Charmonium states are usually assumed to be formed before QGP reaching local equilibrium, and then suffer inelastic scatterings and color screening effect when charmonium move through QGP, which results in dissociations and also transitions between different eigenstates (J/ψ , ψ' , χ_c) [14–20]. These eigenstates are finally detected in experiments through the decay into dileptons. At the LHC energies, abundant charm pairs are produced in nuclear collisions which significantly enhances the combination probability of c and \bar{c} to generate new J/ψ s in QGP [21–23] called “regeneration”. As most of charm quarks are distributed in low and middle p_T region, the regeneration process dominates nuclear modification factor and the collective flows of J/ψ in low and middle p_T bins [24]. In high p_T bin, charmonia are mainly from the initial hadronic collisions [10].

More experimental data about charmonium excited state $\psi(2S)$ have been measured at $\sqrt{s_{NN}} = 2.76$ TeV [25] and 5.02 TeV [26] Pb-Pb collisions in different centralities and transverse momentum bins. $R_{AA}^{\psi(2S)}/R_{AA}^{J/\psi}$ are presented with large discrepancies at these two colliding energies. At 2.76 TeV, $R_{AA}^{\psi(2S)}/R_{AA}^{J/\psi}$ becomes larger than unity in the most central collisions in $3 < p_T < 30$ GeV/c. At 5.02 TeV, the ratio is around ~ 0.5 in a similar centrality and momentum bin. Both of the experimental data carry large error bars, which may prevent any solid conclusions. Different from J/ψ , $\psi(2S)$ is a loosely bound state. Its wavefunction is significantly modified by the hot medium which makes its dissociation and regeneration rates a little indistinct in the hot medium. With smaller binding energy, $\psi(2S)$ is thermally produced in the lower temperature region than J/ψ and inherits larger collective flows from the bulk medium [17, 27, 28]. This sequential regeneration can affect the p_T dependence of the ratio $R_{AA}^{\psi(2S)}/R_{AA}^{J/\psi}$.

In this work, I employ the two-component transport model to study both J/ψ and $\psi(2S)$ production in different centralities and momentum bins at $\sqrt{s_{NN}} = 5.02$ TeV Pb-Pb collisions. I updated the decay rates of excited states with a more realistic formula instead of a survival temperature T_d above which no charmonia can survive. This improvement can explain well the ratio of $\psi(2S)/J/\psi$ at 5.02 TeV Pb-Pb collisions. In Sec.II, I introduce the details of improved Boltzmann transport model for charmonium evolutions and hydrodynamic equations for QGP expansion. In Sec. III, realistic calculations for J/ψ and $\psi(2S)$ at $\sqrt{s_{NN}} = 5.02$ TeV Pb-Pb collisions are presented and compared with the experimental data. A final summary is given in Sec. IV.

II. TRANSPORT MODEL AND HYDRODYNAMICS

Heavy quarkonium evolutions in phase space have been well studied in the hot deconfined medium with Boltzmann transport models from SPS [9] to the LHC [29, 30] in both p-Pb and Pb-Pb collisions. Focusing on hot medium effects, one can start quarkonium evolutions after their hard production. Three-dimensional transport equation for

charmonium evolutions is simplified as,

$$\left[\cosh(y - \eta) \frac{\partial}{\partial \tau} + \frac{\sinh(y - \eta)}{\tau} \frac{\partial}{\partial \eta} + \mathbf{v}_T \cdot \nabla_T \right] f_\Psi = -\alpha_\Psi f_\Psi + \beta_\Psi \quad (1)$$

f_Ψ is the Ψ phase space density. y and η are the rapidities in momentum and coordinate space. $\mathbf{v}_T = \mathbf{p}_T/E_T = \mathbf{p}_T/\sqrt{m_\Psi^2 + p_T^2}$ is the transverse velocity of charmonium, which represents leakage effect in the cooling system with a finite size, i.e., charmonia with a large velocity tend to escape from the thermal medium instead of being dissociated. Primordially produced charmonia in the initial hadronic collisions suffer color screening effects and parton inelastic scatterings, both included in the decay rate α_Ψ ,

$$\alpha_\Psi = \frac{1}{E_T} \int \frac{d^3k}{(2\pi)^3 E_g} \sigma_{g\Psi}(\mathbf{p}, \mathbf{k}, T) F_{g\Psi}(\mathbf{p}, \mathbf{k}) f_g(\mathbf{k}, T) \quad (2)$$

where E_g and f_g are gluon energy and density in the thermal medium. $F_{g\Psi}$ is the flux factor. In the expanding QGP, u^μ represents four velocity of the fluid. Gluon- Ψ cross section in vacuum is extracted from the perturbative calculation with the Coulomb potential approximation. In the thermal medium, I follow Ref.[9] and take a similar form with a reduced binding energy for charmonium,

$$\sigma_{g\Psi}(w) = A_0 \frac{(w/\epsilon_\Psi - 1)^{3/2}}{(w/\epsilon_\Psi)^5} \quad (3)$$

with $A_0 = (2^{11}\pi/27)(m_c^3\epsilon_\Psi)^{-1/2}$ and ϵ_Ψ to be the binding energy of Ψ . Charm quark mass is taken as the mass of D meson to fit the binding energy of charmonium in vacuum. $w = p_\Psi^\mu p_{g\mu}/m_\Psi$ is the gluon energy in Ψ rest frame. In Fig.1, J/ψ decay rate α_Ψ is compared with the quasifree dissociation [27]. Most of J/ψ s can survive in the relatively low temperature region, then two transport models with these decay rates present similar final results in $T < 300$ MeV where most of QGP and charmonia are located [7, 30].

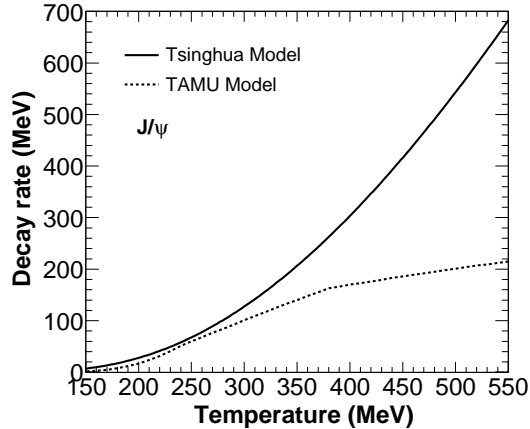


FIG. 1: J/ψ decay rate in the thermal medium as a function of temperature T . Decay rate from quasifree dissociation is plotted for comparison. Solid line is from the improved version of transport model developed by TSINGHUA Group [9, 10, 31], and dotted line is from the calculation of TAMU Group [6, 7, 27].

Heavy quark potential $V(r, T)$ can be screened partially in the thermal medium, especially at the large distance and high temperature supported by Lattice QCD calculations [32]. Charmonium bound states may disappear sequentially in the static medium. The maximum survival temperature of a certain bound state is called “dissociation temperature” T_d , above which this bound state disappears. In nuclear collisions, assuming no bound states can survive at $T > T_d$ strongly suppresses the $\psi(2S)$ production where no excited states can survive inside QGP at $T > T_d^{\chi_c, \psi(2S)} \approx 1.1T_c$. As in the fast cooling system, charmonium states may also survive from the region $T > T_d$ as long as the medium cools down fast below T_d . In this work, I replace the approximation of $\alpha_\Psi(T > T_d) = +\infty$ employed in [33] with a large but finite value, shown in Fig.1. The new decay rate enhances the survival probability of excited states, and weakly affects J/ψ production because of its large T_d . $\psi(2S)$ decay rate is extracted by the geometry scale, $\alpha_{\psi(2S)} = \alpha_{J/\psi} \times \langle r \rangle_{\psi(2S)}^2 / \langle r \rangle_{J/\psi}^2$, similar for χ_c . Mean radius of charmonia in vacuum is calculated with potential model $\langle r \rangle_{J/\psi, \chi_c, \psi(2S)} = (0.5, 0.72, 0.9)$ fm [14].

At the LHC energies, many charm pairs are also produced in Pb-Pb collisions which can significantly enhance the recombination of uncorrelated charm and anti-charm quark in the QGP. This process is included in Eq.(1) with a term β_Ψ . The regeneration rate depends on both charm and anti-charm quark densities in the QGP, and also their recombination probability. At high temperature, charmonium binding energies are reduced significantly which suppresses the generation probability of charmonium. As $\psi(2S)$ is loosely bound, they are thermally produced in the hadronization of QGP. Charm quarks with color charge strongly couple with QGP and suffer energy loss. At relativistic heavy ion collisions, large quench factor and collective flows for charmed mesons have been observed [34–36]. Therefore, one can approximately take kinetically thermalized phase space distribution for charm quarks at $\tau \geq \tau_0$ where τ_0 is the time scale of QGP local equilibrium [37]. As heavy quarks are barely produced from the thermal medium due to its large mass, total number of charm pairs is conserved with spatial diffusions inside QGP [38]. The spatial density is controlled by the conservation equation.

$$\partial_\mu(\rho_c u^\mu) = 0 \quad (4)$$

The initial charm density at τ_0 is obtained by nuclear geometry,

$$\rho_c(\mathbf{x}_T, \eta, \tau_0) = \frac{d\sigma_{pp}^{c\bar{c}}}{d\eta} \frac{T_A(\mathbf{x}_T)T_B(\mathbf{x}_T - \mathbf{b}) \cosh(\eta)}{\tau_0} \quad (5)$$

where T_A and T_B are thickness functions of two colliding nuclei, with the definition of $T_{A(B)}(\mathbf{x}_T) = \int_{-\infty}^{\infty} dz \rho_{A(B)}(\mathbf{x}_T, z)$. $\rho_{A(B)}(\mathbf{x}_T, z)$ is taken as Woods-Saxon nuclear density. The rapidity distribution of charm pairs in $\sqrt{s_{NN}} = 5.02$ TeV pp collisions is obtained by the interpolation of the experimental data at 2.76 TeV and 7 TeV, $d\sigma_{pp}^{c\bar{c}}/dy = 0.86$ mb in the central rapidity $|y| < 0.9$ and 0.56 mb in the forward rapidity $2.5 < |y| < 4$ [39].

The momentum distribution of charmonium primordial production in AA collisions is scaled from the distribution in pp collisions. The parametrization of charmonium initial distribution at 5.02 TeV is similar to the form at 2.76 TeV,

$$\frac{d^2\sigma_{pp}^{J/\psi}}{dy 2\pi p_T dp_T} = f_{J/\psi}^{\text{Norm}}(p_T|y) \cdot \frac{d\sigma_{pp}^{J/\psi}}{dy} \quad (6)$$

$$f_{J/\psi}^{\text{Norm}}(p_T|y) = \frac{(n-1)}{\pi(n-2)\langle p_T^2 \rangle_{pp}} \left[1 + \frac{p_T^2}{(n-2)\langle p_T^2 \rangle_{pp}} \right]^{-n} \quad (7)$$

Charmonium rapidity differential cross section at 5.02 TeV is $d\sigma_{pp}^{J/\psi}/dy = 5.0 \mu\text{b}$ in central rapidity $|y| < 1$ and $3.25 \mu\text{b}$ in the forward rapidity $2.5 < |y| < 4$, through the interpolation between the experimental data of 2.76 TeV [40] and 7 TeV [41] pp collisions. $f_{J/\psi}^{\text{Norm}}(p_T|y)$ is the normalized transverse momentum distribution of charmonium with rapidity y . The mean transverse momentum square $\langle p_T^2 \rangle$ and the parameter n is extracted to be $\langle p_T^2 \rangle_{pp}|_{y=0} = 12.5 (\text{GeV}/c)^2$ and $n = 3.2$. For charmonium momentum distribution in other rapidities, lack of more constraints, $\langle p_T^2 \rangle_{pp}(y)$ is determined by the relation,

$$\langle p_T^2 \rangle_{pp}^{J/\psi}(y) = \langle p_T^2 \rangle_{pp}^{J/\psi}|_{y=0} \times \left[1 - \left(\frac{y}{y_{\text{max}}} \right)^2 \right] \quad (8)$$

where $y_{\text{max}} = \cosh^{-1}(\sqrt{s_{NN}}/(2E_T))$ is the maximum rapidity of charmonium in pp collisions with zero transverse momentum. As the masses of charmonium excited states ($\chi_c, \psi(2S)$) are close to J/ψ , their initial momentum distributions are approximated to be the same with Eq.(6-7).

In nuclear collisions, charmonium initial distribution is also modified by the shadowing effects in the nucleus [42, 43]. I employ the EPS09 NLO model [44] to generate the modification factors for primordially produced charmonium at $\sqrt{s_{NN}} = 5.02$ TeV Pb-Pb collisions. This suppression factor is roughly ~ 0.8 depending on the impact parameter. For the regeneration, shadowing effect reduces the number of charm pairs by around 20%, and suppress the regeneration by a factor of $\sim 0.8^2$.

QGP expansion as a background for charmonium evolutions is simulated with the (2+1) dimensional ideal hydrodynamic equations in the transverse plane, with the assumption of Bjorken expansion in longitudinal direction.

$$\partial_\mu T^{\mu\nu} = 0 \quad (9)$$

$T^{\mu\nu} = (e+p)u^\mu u^\nu - g^{\mu\nu}p$ is the energy-momentum tensor. e and p are the energy density and the pressure. u^μ is the four velocity of QGP fluids, which can affect charm spatial diffusions through Eq.(4) and the charmonium regeneration. It also determines the collective flows of light hadrons, charmed mesons and the regenerated charmonia. The deconfined matter is treated as an ideal gas of massless gluons, u and d quarks, and strange quark with mass

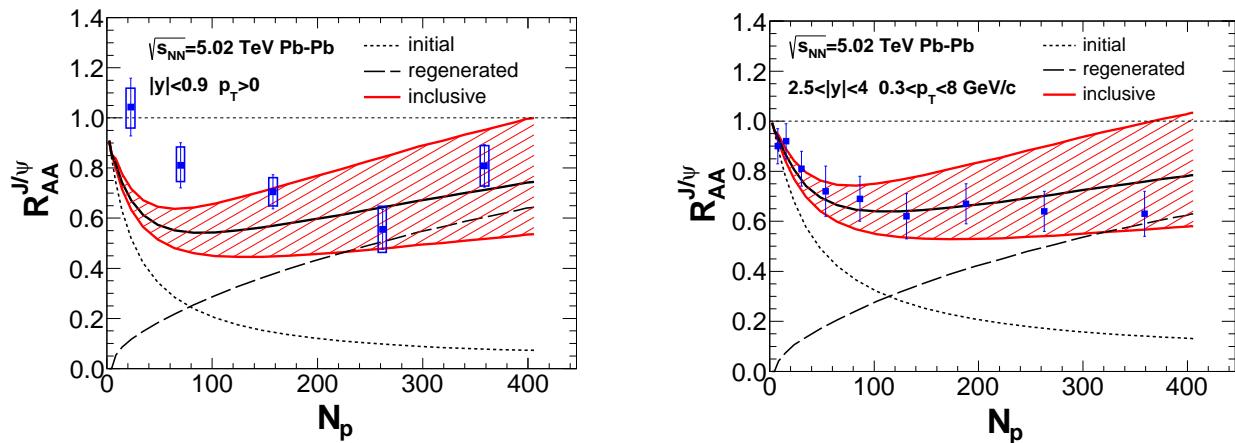


FIG. 2: (Left panel) inclusive nuclear modification factor R_{AA} of J/ψ as a function of the number of participants N_p in central rapidity in Pb-Pb collisions at $\sqrt{s_{NN}} = 5.02$ TeV. The dotted and dashed lines are the primordial production and regeneration respectively. Black solid line in the middle of the band is for J/ψ inclusive R_{AA} . Color band is for the uncertainties of the inputs, with $d\sigma_{pp}^{c\bar{c}}/dy$ changed by $\pm 20\%$. Experimental data is from ALICE Collaboration [47]. (Right panel) inclusive R_{AA} in forward rapidity. The lines and the band are similar to the left panel. Experimental data is from ALICE Collaboration [48].

$m_s = 150$ MeV [45]. Hadron gas is an ideal gas of all known hadrons and resonances with mass up to 2 GeV [46]. Two phases are connected with first-order phase transition and the critical temperature is $T_c = 170$ MeV. The initial maximum temperature of QGP is extracted to be $T_0(\mathbf{x}_T = 0, \tau_0) = 510$ MeV in the central rapidity $|y| < 2.4$ and 450 MeV in the forward rapidity $2.5 < |y| < 4$. Here $\tau_0 = 0.6$ fm/c is the time scale of QGP reaching local equilibrium [37]. The lifetime of QGP is ~ 10 fm/c in the most central Pb-Pb collisions at $\sqrt{s_{NN}} = 5.02$ TeV.

III. NUMERICAL RESULTS AND ANALYSIS

With the transport model for charmonium evolutions and hydrodynamic equations for QGP collective expansion, one can obtain the realistic nuclear modification factors of charmonia in the heavy ion collisions. In the left panel of Fig.2, primordially produced charmonia suffer dissociations from peripheral to central Pb-Pb collisions, plotted with the dotted line. The regeneration from $c + \bar{c} \rightarrow J/\psi + g$ is plotted with dashed line which is proportional to the number of charm pairs in QGP, and dominates J/ψ total production in the central collisions. The experimental data in left panel of Fig.2 is inclusive production which includes the non-prompt part from B-hadron decays. It contributes around 10% to the final inclusive yields. Detailed momentum dependence of non-prompt fraction in J/ψ inclusive production is fitted as $f_B = N_{pp}^{B \rightarrow J/\psi} / (N_{pp}^{\text{prompt}} + N_{pp}^{B \rightarrow J/\psi}) = 0.04 + 0.023 p_T / (\text{GeV}/c)$ [33], with weak dependence on rapidity and the colliding energies $\sqrt{s_{NN}}$. In nuclear collisions, bottom quarks suffer strong energy loss in the thermal medium. B hadrons and non-prompt charmonia are shifted from high p_T to relatively low p_T . This hot medium modification on non-prompt charmonium (or bottom quark) momentum distribution is characterized with a quench factor R_Q . In high p_T , quench factor R_Q is smaller than unity, extracted to be 0.4 from non-prompt J/ψ R_{AA} [33]. This value is also employed in the entire p_T region. With both prompt and non-prompt charmonia, one can obtain charmonium inclusive nuclear modification factors in Fig.2. Considering large uncertainties of $d\sigma_{pp}^{c\bar{c}}/dy$ in the transport model, I perform two calculations for R_{AA} with the change of $d\sigma_{pp}^{c\bar{c}}/dy$ by $\pm 20\%$, see the color band in Fig.2. In most central collisions, primordial production is strongly suppressed and regeneration dominates the total yield.

In the forward rapidity, both initial conditions of hydrodynamic equations and the transport model are updated properly compared with the central rapidity collisions. In the right panel of Fig.2, J/ψ nuclear modification factor from the primordial production (dotted line), regeneration (dashed line), and the inclusive production (color band) are plotted separately. The flat tendency of experimental data with N_p is due to the combined effects of the decrease of primordial production and the increase of regeneration in final J/ψ yield. The experimental data in the right panel of Fig.2 is at $0.3 < p_T < 8$ GeV/c. It can exclude the contribution of coherent photoproduction which are distributed below 0.3 GeV/c. The additional contribution from charmonium coherent photoproduction can make total R_{AA} larger than unity in ultra-peripheral collisions [31].

In order to show the contributions of primordial production and regeneration, the p_T -differential R_{AA} is also plotted

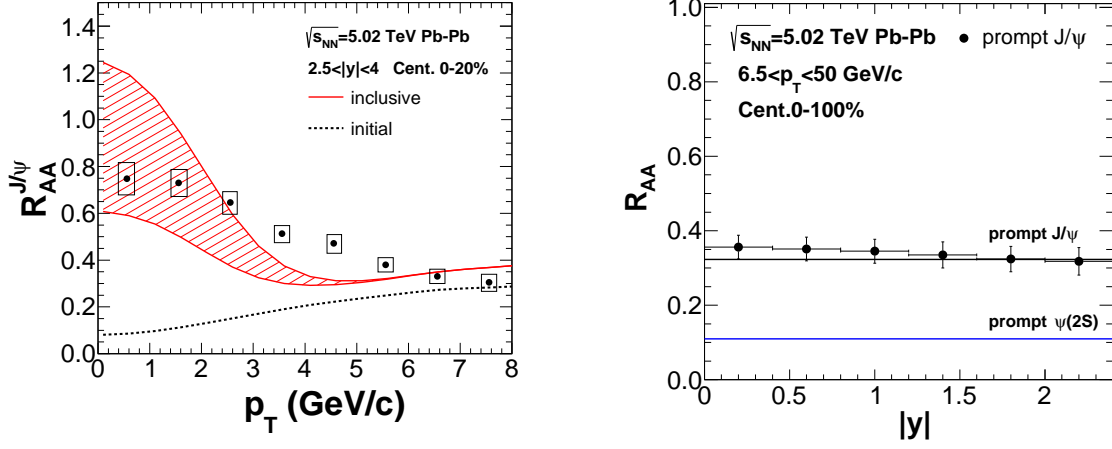


FIG. 3: (Color online) (Left panel) J/ψ nuclear modification factor R_{AA} as a function of transverse momentum p_T . Dotted line is for initial production, solid line is for inclusive production consisting of initial production, regeneration and B hadron decay. Color band is due to the uncertainties of $d\sigma_{pp}^{c\bar{c}}/dy$ (see Fig.2). Difference between solid line and dotted line is mainly due to the contribution of regeneration at low p_T and B hadron decay at high p_T respectively. Experimental data is from ALICE Collaboration [49]. (Right panel) J/ψ prompt R_{AA} as a function of rapidity in the centrality 0-100%. $\psi(2S)$ prompt $R_{AA}(y)$ is also predicted. The experimental data are from [50].

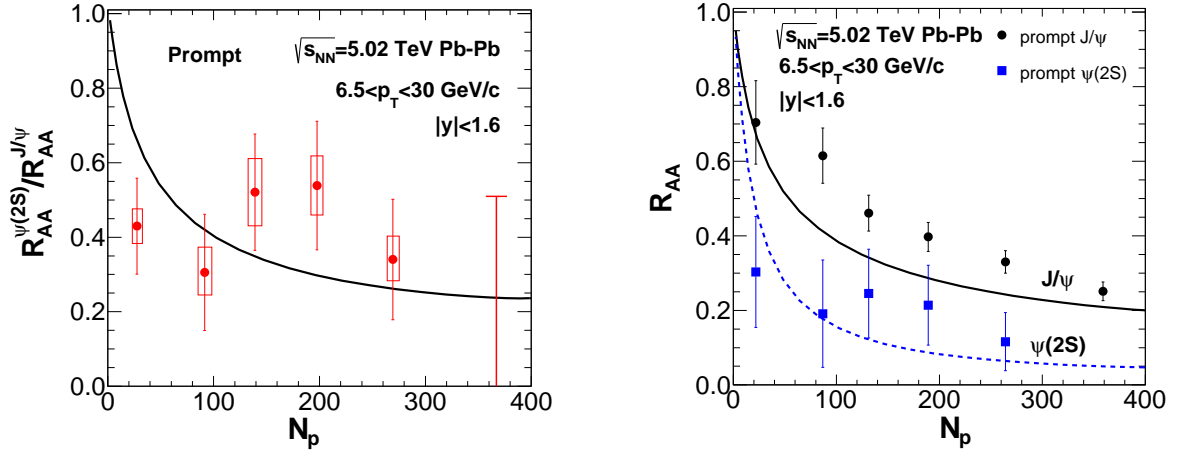


FIG. 4: (Color online) (Left panel) the ratio of J/ψ and $\psi(2S)$ prompt nuclear modification factors in central rapidity region with a momentum cut $6.5 < p_T < 30$ GeV/c in $\sqrt{s_{NN}} = 5.02$ TeV Pb-Pb collisions. Experimental data are from CMS Collaboration [26]. (Right panel) J/ψ and $\psi(2S)$ prompt nuclear modification factor as a function of N_p in central rapidity region with a momentum cut $6.5 < p_T < 30$ GeV/c in $\sqrt{s_{NN}} = 5.02$ TeV Pb-Pb collisions. The experimental data are from [50].

in left panel of Fig.3. Significant enhancement of R_{AA} in the low p_T region is caused by the regeneration. Large suppression in high p_T region is due to the color screening and parton inelastic collisions. Dotted line is for the initial production, it increases slightly with p_T due to the leakage effect. Both theoretical results of $R_{AA}^{J/\psi}$ in central and forward rapidities can explain experimental data well. Note that even the charm pair cross section $d\sigma_{pp}^{c\bar{c}}/dy$ in central rapidity is larger than the value in forward rapidity, R_{AA} is similar to each other in two rapidities. Because in central rapidity with hotter medium, QGP strong expansion “blows” charm quarks to a larger volume, which suppresses the charm quark spatial density and the charmonium regeneration. Meanwhile, the elliptic flows of regenerated charmonia become larger in the central rapidity. These will be discussed in details below. In the right panel of Fig.3, J/ψ and $\psi(2S)$ prompt R_{AA} as a function of rapidity is also presented.

Situation becomes a little complicated for $\psi(2S)$ in the hot medium because of its dissociation rate compared with the tightly bound J/ψ . $\psi(2S)$ decay rate here is extracted from J/ψ by the geometry scale in Section II. In

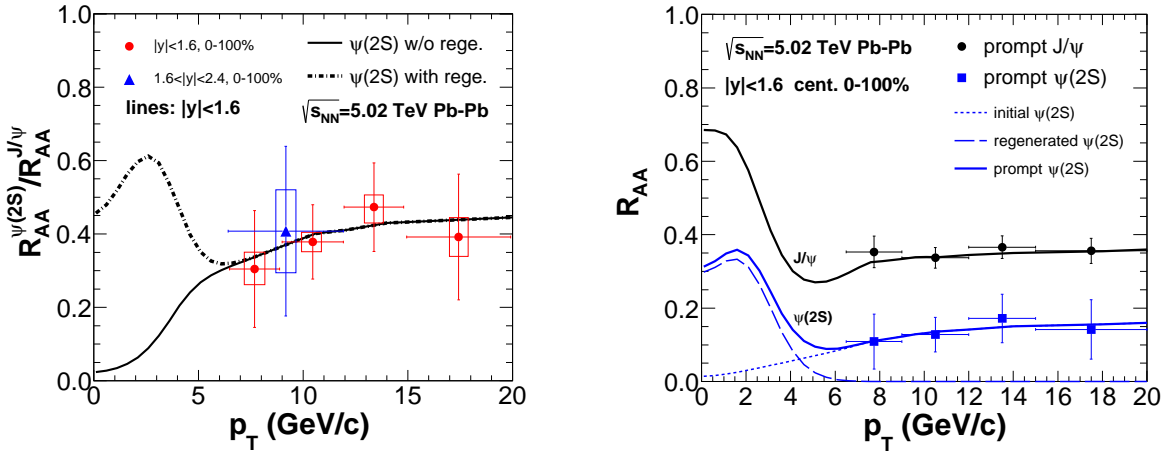


FIG. 5: (Color online) (Left panel) Ratio of J/ψ and $\psi(2S)$ prompt nuclear modification factors as a function of the transverse momentum p_T in the minimum bias (corresponding to the impact parameter $b=8.4$ fm) at $\sqrt{s_{NN}} = 5.02$ TeV Pb-Pb collisions. Dotted-dashed and solid lines are with and without $\psi(2S)$ regeneration, respectively. Experimental data are from CMS Collaboration [26, 50]. (Right panel) J/ψ and $\psi(2S)$ nuclear modification factor as a function of transverse momentum. Black dotted, dashed and solid lines are for initial, regenerated and prompt $\psi(2S)$ respectively. Prompt $R_{AA}^{J/\psi}$ is also plotted for comparison. The experimental data are from [26, 50].

Fig.4, charmonia with high p_T are mainly from the primordial production. From peripheral to central collisions, $\psi(2S)$ suffers stronger dissociation and the ratio of $R_{AA}^{\psi(2S)}/R_{AA}^{J/\psi}$ decreases with N_p . In the most central collisions at LHC, the ratio of charmonium nuclear modification factors is proportional to their decay rates. In peripheral collisions, charmonium path length in hot medium becomes smaller. With weak suppression, J/ψ and $\psi(2S)$ nuclear modification factors approach unity, which makes $R_{AA}^{\psi(2S)}/R_{AA}^{J/\psi} \rightarrow 1$ at $N_p \rightarrow 2$, see left panel of Fig.4. Individual $R_{AA}^{J/\psi}$ in high p_T bin is also plotted in the right panel of Fig.4. The decreasing tendency of J/ψ and $\psi(2S)$ R_{AA} with N_p are explained well.

Transverse momentum dependence of $R_{AA}^{\psi(2S)}/R_{AA}^{J/\psi}$ is also studied based on the sequential regeneration mechanism. In Fig.5, at $p_T \rightarrow 0$, there will be significant regeneration for J/ψ . For loosely bound $\psi(2S)$, they can only be thermally produced in the later stage of QGP expansion compared with J/ψ , which makes regenerated $\psi(2S)$ inherit larger velocity and collective flows from the bulk medium based on the fact of strong couplings between charm quarks and the deconfined medium. Therefore, the regenerated $\psi(2S)$ are distributed in the larger p_T (dashed line in right panel of Fig.5) compared with the regenerated J/ψ . Due to the different p_T distributions of thermally produced J/ψ and $\psi(2S)$, the shapes of J/ψ and $\psi(2S)$ $R_{AA}(p_T)$ s (black and blue solid lines in right panel of Fig.5) are different. There is a “peak” in the ratio $R_{AA}^{\psi(2S)}/R_{AA}^{J/\psi}$ in the left panel of Fig.5 due to the sequential regeneration of $\psi(2S)$. If without $\psi(2S)$ regeneration, the ratio will decrease to zero at $p_T \rightarrow 0$, see the solid line in the left panel of Fig.5.

In the low and middle p_T region, regeneration becomes important for J/ψ and $\psi(2S)$ and enhances their R_{AA} in semi-central and central collisions. In order to show the roles of $\psi(2S)$ regeneration on $R_{AA}^{\psi(2S)}/R_{AA}^{J/\psi}$, we present two calculations with and without $\psi(2S)$ regeneration respectively in Fig.6. In Fig.6, neglecting the regeneration for $\psi(2S)$ (solid line), $R_{AA}^{\psi(2S)}/R_{AA}^{J/\psi}$ keeps dropping down with N_p due to the stronger QGP suppression on charmonium excited states. The supplement of regeneration increases $\psi(2S)$ production especially in the central collisions and enhances the value of $R_{AA}^{\psi(2S)}/R_{AA}^{J/\psi}$, see the dotted-dashed line. Note that in the work of Ref.[33], predictions about prompt $R_{AA}^{\psi(2S)}/R_{AA}^{J/\psi}$ at 2.76 TeV Pb-Pb collisions have been made. Its value is predicted to be around ~ 0.15 in all p_T bins. The binding energy and the regeneration rate for $\psi(2S)$ in Ref.[33] is smaller which suppress $\psi(2S)$ production. I extend previous calculations from 2.76 TeV [33] to 5.02 TeV, both of them are consistent with the experimental data at 5.02 TeV. The difference between solid and dotted-dashed lines in Fig.6 are due to the $\psi(2S)$ regeneration component.

Further more, the anisotropies of J/ψ and $\psi(2S)$ momentum distributions are also studied in Fig.7. Charmonia moving inside QGP likely as a color neutral bound state, are weakly coupled with the bulk medium, and therefore less affected by the collective expansions of QGP compared with open charm quarks. The non-zero elliptic flow of primordially produced J/ψ at $p_T > 6$ GeV/c is mainly from the effects of path length difference in the transverse plane, see the solid line in left panel of Fig.7. At the low p_T , J/ψ production is dominated by the regeneration. These

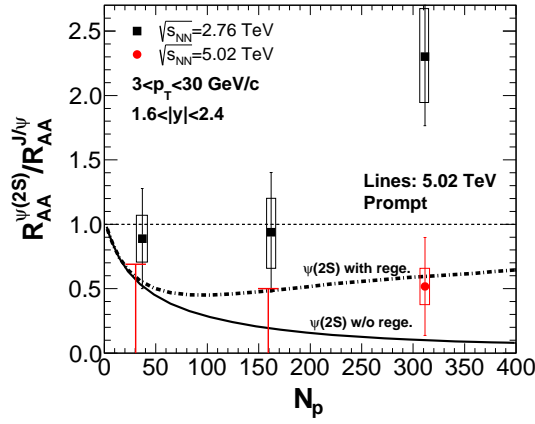


FIG. 6: (Color online) Ratio of J/ψ and $\psi(2S)$ prompt nuclear modification factors as a function of N_p in rapidity $1.6 < |y| < 2.4$ with a momentum cut $3 < p_T < 30$ GeV/c. Dotted-dashed line is the scenario for J/ψ and $\psi(2S)$ with both primordial production and regeneration, solid line is the scenario without regeneration for $\psi(2S)$ (J/ψ regeneration is included in both lines). Experimental data at $\sqrt{s_{NN}} = 2.76$ TeV and 5.02 TeV are from CMS Collaboration [26].

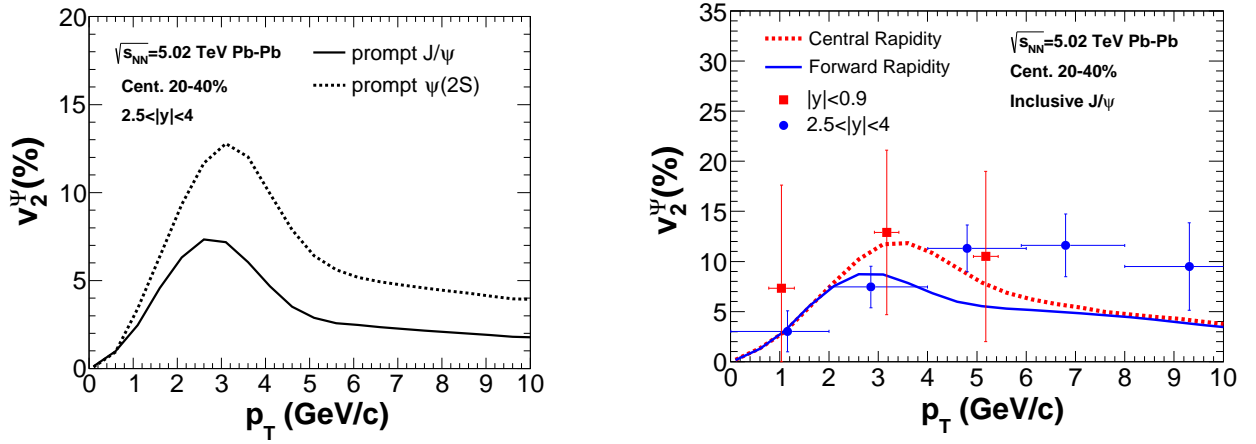


FIG. 7: (Color online) (Left panel) Elliptic flows of prompt J/ψ and $\psi(2S)$ as a function of transverse momentum p_T in centrality 20-40% in the forward rapidity $2.5 < |y| < 4$ $\sqrt{s_{NN}} = 5.02$ TeV Pb-Pb collisions. Solid and dotted lines are for the prompt J/ψ and $\psi(2S)$. (Right panel) Elliptic flows of inclusive J/ψ as a function of transverse momentum p_T . Solid line and dotted line are for the inclusive J/ψ in forward and central rapidities. Experimental data is from ALICE Collaboration [51].

heavy quarks are strongly coupled with the thermal medium and inherit collective flows, which results in a peak of v_2 at $p_T \sim 3$ GeV/c. The elliptic flows of prompt $\psi(2S)$ are also presented with dotted line. As $\psi(2S)$ is regenerated in the later stage of QGP anisotropic expansions, their elliptic flow is larger than J/ψ . In the high p_T region, the momentum anisotropy of $\psi(2S)$ is larger than J/ψ , as they are easily dissociated and sensitive to the anisotropy of the bulk medium.

In right panel of Fig.7, the experimental data is for inclusive J/ψ including non-prompt contribution from B hadron decay. The solid line is for inclusive J/ψ assuming kinetic equilibrium for bottom quarks as an up-limit [30]. Non-prompt part becomes important at high p_T and therefore kinetically thermalized bottom quarks can enhance the inclusive $v_2^{J/\psi}$ by $\sim 2\%$ at $p_T \sim 8$ GeV/c. $v_2^{J/\psi}$ in central rapidity is also calculated with dotted line for comparison. For the situation of inclusive $\psi(2S)$, it is connected with the energy loss of bottom quarks in QGP, and has been elaboratively studied in Ref.[33].

IV. SUMMARY

In summary, this work employs the improved transport model to study the thermal production of J/ψ and $\psi(2S)$ in Pb-Pb collisions at $\sqrt{s_{NN}} = 5.02$ TeV. Charmonium nuclear modification factors are dominated by the regeneration at low p_T and the primordial production at high p_T respectively. With different binding energies, J/ψ and $\psi(2S)$ can be sequentially produced in the different stage of QGP anisotropic expansions. This results in different p_T distributions of regenerated J/ψ and $\psi(2S)$. We explain well both J/ψ and $\psi(2S)$ R_{AA} and their ratio at 5.02 TeV Pb-Pb collisions. This clearly shows how the open charm quark evolutions can affect the final charmonium productions. The sequential regeneration of J/ψ and $\psi(2S)$ contains the histories of charm quark diffusions and QGP expansions in heavy-ion collisions.

Acknowledgement: I acknowledge instructive discussions with Prof. Pengfei Zhuang and Jiaying Zhao. I am also grateful to Prof. Carsten Greiner for the kind hospitality during this study. This work is supported by NSFC Grant No. 11705125 and Sino-Germany (CSC-DAAD) Postdoc Scholarship.

-
- [1] T. Matsui and H. Satz, Phys. Lett. B **178**, 416 (1986).
 [2] A. Adare *et al.* [PHENIX Collaboration], Phys. Rev. Lett. **98**, 232301 (2007)
 [3] B. Abelev *et al.* [ALICE Collaboration], Phys. Rev. Lett. **109** (2012) 072301
 [4] S. Chatrchyan *et al.* [CMS Collaboration], JHEP **1205**, 063 (2012)
 [5] J. Adam *et al.* [ALICE Collaboration], JHEP **1511**, 127 (2015)
 [6] L. Grandchamp and R. Rapp, Phys. Lett. B **523**, 60 (2001);
 [7] X. Zhao and R. Rapp, Phys. Rev. C **82**, 064905 (2010)
 [8] X. Du and R. Rapp, arXiv:1808.10014 [nucl-th].
 [9] X. l. Zhu, P. f. Zhuang and N. Xu, Phys. Lett. B **607**, 107 (2005);
 [10] B. Chen, Phys. Rev. C **93**, no. 5, 054905 (2016); B. Chen, K. Zhou and P. Zhuang, Phys. Rev. C **86**, 034906 (2012)
 [11] J. P. Blaizot, D. De Boni, P. Faccioli and G. Garberoglio, Nucl. Phys. A **946**, 49 (2016)
 [12] J. P. Blaizot and M. A. Escobedo, Phys. Rev. D **98**, no. 7, 074007 (2018)
 [13] C. Gerschel and J. Hufner, Phys. Lett. B **207**, 253 (1988).
 [14] H. Satz, J. Phys. G **32**, R25 (2006)
 [15] R. Katz and P. B. Gossiaux, Annals Phys. **368**, 267 (2016)
 [16] J. P. Blaizot and M. A. Escobedo, JHEP **1806**, 034 (2018)
 [17] B. Chen, Phys. Rev. C **95**, no. 3, 034908 (2017)
 [18] X. Yao and B. Müller, Phys. Rev. C **97**, no. 1, 014908 (2018) Erratum: [Phys. Rev. C **97**, 049903(E) (2018)]
 [19] X. Yao and T. Mehen, arXiv:1811.07027 [hep-ph].
 [20] X. Yao and B. Müller, arXiv:1811.09644 [hep-ph].
 [21] R. L. Thews, M. Schroedter and J. Rafelski, Phys. Rev. C **63**, 054905 (2001)
 [22] A. Andronic, P. Braun-Munzinger, K. Redlich and J. Stachel, Phys. Lett. B **571**, 36 (2003)
 [23] L. Yan, P. Zhuang and N. Xu, Phys. Rev. Lett. **97**, 232301 (2006)
 [24] X. Zhao and R. Rapp, Nucl. Phys. A **859**, 114 (2011)
 [25] V. Khachatryan *et al.* [CMS Collaboration], Phys. Rev. Lett. **113**, no. 26, 262301 (2014)
 AAAAA
 [26] A. M. Sirunyan *et al.* [CMS Collaboration], Phys. Rev. Lett. **118**, no. 16, 162301 (2017)
 [27] X. Du and R. Rapp, Nucl. Phys. A **943**, 147 (2015)
 [28] J. Zhao and B. Chen, Phys. Lett. B **776**, 17 (2018)
 [29] B. Chen, T. Guo, Y. Liu and P. Zhuang, Phys. Lett. B **765**, 323 (2017)
 [30] K. Zhou, N. Xu, Z. Xu and P. Zhuang, Phys. Rev. C **89** (2014) no.5, 054911
 [31] W. Shi, W. Zha and B. Chen, Phys. Lett. B **777**, 399 (2018)
 [32] Y. Burnier, O. Kaczmarek and A. Rothkopf, Phys. Rev. Lett. **114**, no. 8, 082001 (2015)
 [33] B. Chen, Y. Liu, K. Zhou and P. Zhuang, Phys. Lett. B **726**, 725 (2013)
 [34] B. I. Abelev *et al.* [STAR Collaboration], Phys. Rev. Lett. **98**, 192301 (2007) Erratum: [Phys. Rev. Lett. **106**, 159902 (2011)]
 [35] A. Adare *et al.* [PHENIX Collaboration], Phys. Rev. Lett. **98**, 172301 (2007)
 [36] B. Abelev *et al.* [ALICE Collaboration], Phys. Rev. Lett. **111**, 102301 (2013)
 [37] W. Zhao, H. j. Xu and H. Song, Eur. Phys. J. C **77**, no. 9, 645 (2017)
 [38] J. Zhao, S. Shi, N. Xu and P. Zhuang, arXiv:1805.10858 [hep-ph].
 [39] R. Aaij *et al.* [LHCb Collaboration], JHEP **1706**, 147 (2017)
 [40] B. Abelev *et al.* [ALICE Collaboration], Phys. Lett. B **718**, 295 (2012) Erratum: [Phys. Lett. B **748**, 472 (2015)]
 [41] B. Abelev *et al.* [ALICE Collaboration], JHEP **1211**, 065 (2012)
 [42] R. Vogt, Phys. Rev. C **71**, 054902 (2005)

- [43] K. J. Eskola, V. J. Kolhinen and C. A. Salgado, *Eur. Phys. J. C* **9**, 61 (1999)
- [44] K. J. Eskola, H. Paukkunen and C. A. Salgado, *JHEP* **0904**, 065 (2009)
- [45] J. Sollfrank, P. Huovinen, M. Kataja, P. V. Ruuskanen, M. Prakash and R. Venugopalan, *Phys. Rev. C* **55**, 392 (1997)
- [46] C. Patrignani *et al.* [Particle Data Group], *Chin. Phys. C* **40**, no. 10, 100001 (2016).
- [47] R. T. Jimnez Bustamante [ALICE Collaboration], *Nucl. Phys. A* **967**, 576 (2017).
- [48] J. Adam *et al.* [ALICE Collaboration], *Phys. Lett. B* **766**, 212 (2017)
- [49] B. Paul [ALICE Collaboration], *J. Phys. Conf. Ser.* **779**, no. 1, 012037 (2017)
- [50] A. M. Sirunyan *et al.* [CMS Collaboration], *Eur. Phys. J. C* **78**, no. 6, 509 (2018)
- [51] S. Acharya *et al.* [ALICE Collaboration], *Phys. Rev. Lett.* **119**, no. 24, 242301 (2017)